Energy-based numerical evaluation for seismic performance of a high-rise steel building

H.D. Zhang[*1] and Y.F. Wang[2]

1School of Civil Engineering, Tianjin Institute of Urban Construction, Tianjin, PR China
2School of Civil Engineering, Beijing Jiaotong University, Beijing, PR China

Abstract.   As an alternative to current conventional force-based assessment methods, the energy-based seismic performance of a code-designed 20-storey high-rise steel building is evaluated in this paper. Using 3D nonlinear dynamic time-history method with consideration of additional material damping effect, the influences of different restoring force models and P-Δ/δ effects on energy components are investigated. By combining equivalent viscous damping and hysteretic damping ratios of the structure subjected to strong ground motions, a new damping model, which is amplitude-dependent, is discussed in detail. According to the analytical results, all energy components are affected to various extents by P-Δ/δ effects and a difference of less than 10% is observed; the energy values of the structure without consideration of P-Δ/δ effects are larger, while the restoring force models have a minor effect on seismic input energy with a difference of less than 5%, but they have a certain effect on both viscous damping energy and hysteretic energy with a difference of about 5~15%. The paper shows that the use of the hysteretic energy at its ultimate state as a seismic design parameter has more advantages than seismic input energy since it presents a more stable value. The total damping ratio of a structure consists of viscous damping ratio and hysteretic damping ratio and it is found that the equivalent viscous damping ratio is a constant for the structure, while the equivalent hysteretic damping ratio approximately increases linearly with structural response in elasto-plastic stage.

Keywords: steel structure; numerical evaluation; seismic performance; energy balance concept; restoring force model; P-Δ/δ effects; damping model.

1. Introduction

In current seismic design codes in most of countries, structural design is achieved by performing a force-based demand-capacity analysis. It is well known that the structural seismic performance is related, not only to the maximum responses, but also to the seismic input energy and inelastic energy dissipation of a structure. In fact, the earthquake action on building structures is a time-history procedure, and the seismic input energy imparted to structures is finally dissipated by viscous damping and hysteretic behavior (Jawahar and James 1987). Therefore, the use of energy method for evaluating the seismic performance of a structure is more realistic and rational.

New trends in the seismic design methodologies are oriented to the definition of performance- based methods for the design of new facilities and for the assessment of the seismic capacity of existing

---

facilities (Gaetano 2001). In the last few years, the energy balance method has been largely accepted for assessing the seismic capacity of existing structures (Safac 2000, Decanini and Mollaioli 2001, Fajfar and Vidic 1994, Choi and Kim 2009). Leelataviwat *et al.* (2002) adopted the energy balance concept to derive seismic design forces for SDOF (single degree-of-freedom) systems and the method also was extended to derive the design forces for multistory frames. In order to understand the variation in energy demand for various structures, energy spectra were constructed by using SDOF systems (Fajfar *et al.* 1989). Somerville *et al.* (1997) used sixty recorded earthquake excitations to compute the seismic energy demands of multi-story and equivalent SDOF structures. The energy balance concept also has been adopted by other researchers (Bojórquez *et al.* 2008, Reyes-Salazar and Haldar 2001) to develop energy-based methodologies that aim at providing earthquake-resistant structures with an energy dissipating capacity larger than or equal to its corresponding demand.

However, research conducted by Fajfar and Gašperšič (1996), Shen and Akbas (1999) showed that the hysteretic energy demand in an MDOF (multiple degree-of-freedom) system cannot be reliably evaluated from an equivalent SDOF system. One of the difficulties involved in assessing the energy demand in MDOF systems is to predict the energy distribution along the height of structures in which the higher mode effects play an important role. Taking the higher mode effects into consideration, Chou and Uang (2003) proposed a method for estimating the first and the second "modal" absorbed energies of symmetric-plan multi-storey buildings. Using the modal pushover analysis (MPA) methods (Chopra and Goel 2002), Prasanth *et al.* (2008) computed the hysteretic energy components of the first few vibration "modes" of symmetric-plan multi-storey buildings and summed together as the estimated total hysteretic energy of the buildings.

There are many important factors affecting the energy components of a structure subjected to strong ground motion, such as restoring force models, P-Δ/δ effects and damping characteristics. The influences of the factors on the analysis results should be evaluated.

In this paper, the energy-based dynamic behaviors of a spatial moment resisting steel frame are investigated by means of non-linear time-history method, and the main factors affecting energy components and relevant parameters are discussed in detail.

2. Numerical model based on energy balance concept

The dynamic equation of an inelastic SDOF system subjected to a horizontal ground motion can be written as follows

$$m\ddot{y} + C\dot{y} + Q(y) = -m z_g \tag{1}$$

where m is the mass; y is the relative displacement of the mass; C is the damping coefficient and $Q(y)$ is the restoring force and z_g is the ground acceleration. The dots in the variables indicate the derivates with respect to time t. Integrating Eq. (1) with respect to y from the time that ground motion starts, the energy balance equation is as follow (Chopra 1995)

$$E_k + E_\xi + E_a = E_I \tag{2}$$

in which

$$E_k = \frac{m\dot{y}^2}{2}; E_\xi = \int C\dot{y}^2 dt; E_a = \int Q(y)\dot{y} dt; E_I = \int m z_g dy \qquad (3)$$

where, E_k is the kinetic energy, E_ξ is the viscous damping energy, E_a is the dissipated energy. E_I is, by definition, the relative seismic energy input. E_a is composed of the recoverable elastic strain energy, E_s, and the irrecoverable hysteretic energy E_h, i.e., $E_a = E_s + E_h$, then Eq. (2) is rewritten

$$E_k + E_\xi + E_s + E_h = E_I \qquad (4)$$

Eq. (4) also holds for MDOF systems, i.e., an N-storey building, if the scalars are replaced by the corresponding matrix and vectors.

The energy in Eq. (4) is the relative energy based on the relative displacement between the structure and the base. The absolute energy can be estimated using the absolute displacement, but the absolute energy method has some practical shortcomings (Bruneau 1996). By comparing the absolute energy with the relative energy time histories for a SDOF structure, Akiyama (2010) considered the relative energy more meaningful from the viewpoint of engineering interest.

The left-hand side of Eq. (4) is interpreted as the seismic capacity of the structure and the right-hand side represents the loading effect of the earthquake in terms of the input energy. Results obtained by the previous researchers, such as Fajfar and Fischinger (1990) and Zahrah and Hall (1984), have indicated that the maximum input energy per unit mass has a relatively stable value in the region of the predominant period of the ground motion. Thus, the seismic safety of the structure can be assessed by comparing the expected value of E_I at the site where the building is located with its seismic capacity. The design requirements of an earthquake-resistant structure can be formulated as follows

$$\alpha_I = E_{I, demand} / E_{I, capacity} \le 1 \qquad (5)$$

in which α_I = demand-capacity ratio of seismic input energy.

However, among the energy components absorbed and dissipated by a structure, researchers (Uang and Bertero 1990, Bojórquez *et al.* 2010) demonstrated that the plastic hysteretic energy, E_h, is clearly related to structural damage and E_h can be physically interpreted by considering that it is equal to the total area under all the hysteresis loops that a structure undergoes during a ground motion. Therefore, it is convenient to express Eq. (5) in terms of plastic hysteretic energy

$$\alpha_h = E_{h, demand} / E_{h, capacity} \le 1 \qquad (6)$$

3. Main factors affecting energy components

According to Eqs. (1) and (3), the main factors which affect energy demands are damping and restoring force models, meanwhile, P-Δ/δ effects also cannot be ignored for the high-rise building. These factors are discussed in detail in this paper.

3.1 Damping

The damping in a structure plays an important role in energy dissipation. Most of physical energy

dissipation in real structures is a nonlinear function of structural displacement. Nevertheless, it is common practice to approximate the nonlinear behavior with an "equivalent linear damping" and viscous damping model is the most common form of damping considered in the general MDOF systems. Many of the currently available guidelines regarding to damping are intended for use with elastic dynamic analysis (PEER/ATC 2010). In an inelastic analysis, when the viscous damping model is used, the additional material damping in high stress level, such as post yielding, is not captured by the nonlinear hysteretic response that is explicitly simulated in the model (FEMA 2009b). In order to take additional damping effect into consideration, the viscous damping model in a nonlinear analysis should be modified.

3.2 Restoring force models

Nonlinearity in structural response is often due to the restoring force characteristics of a structure, i.e., variations in structural stiffness and damping during strong earthquakes. Choosing the proper restoring force models for members are usually based on the deformation-force characteristics obtained from static or dynamic loading experiments. However, due to the limited amount of data available, designing a restoring force model based on the data in some available guidelines is very important in civil engineering.

Many structural members or systems will experience reductions in strength when subjected to cyclic loading (FEMA 2009a). Cyclic strength loss increases displacement demands, but it results in reduction of carrying loading (Nassar 1991), and thus further research on the effects of strength loss on energy components is needed before quantitative conclusions could be drawn.

3.3 P-Δ/δ effects

Gravity loads lead to a reduction of the lateral stiffness of columns or buildings. For elastic structural behaviors, the decrease is of minor importance because the magnitude is small compared to the first order elastic stiffness. During strong seismic excitations, however, the inelastic deformation combined with gravity causes a structure or column to lose dynamic stability if the post-yield tangent stiffness becomes negative, which may greatly affect energy dissipation capacity of a structure or member.

Studies of the effect of gravity on the inelastic seismic response and carrying capacity of structures or members have been carried out by many researchers (Williamson 2003, Aschheim 2003, Chen and Wang 1999). However, the influence of P-Δ/δ effects on energy components is less investigated in previous papers.

4. Finite element model of a high-rise steel building

4.1 Details of the high rise steel building

A code-designed high-rise steel frame building is investigated as a practical application. The structural height, length and width are 77.88 m, 30.48 m and 18.3 m, respectively. This building contains 20 stories, and has 3×4 bays in plan and span lengths are 7.62 m and 6.10 m in two directions. The first story height is 5.49 m and typical story height is 3.81 m. The typical floor slab thickness in the structure is 200 mm. The 3D model, typical floor plan, elevation of the structure and cross section are shown in

Figs. 1 to 3.

The floors are subjected to a live load of 2.4 kPa, representing a load of an office building, and a superimposed dead load of 4.5 kPa for the equivalent mechanical loads and the self-weight of the floor. The load combination used in the nonlinear dynamic analysis is 1.0DL + 0.25LL.

Two representative recorded earthquake ground motions are selected as dynamic loads: El-Centro (Imperial Valley 1940/05/19, PGA = 0.2148 g) and Kobe (Kobe 1995/01/16, PGA = −0.6934 g), as shown in Table 1. In order to describe the structural elasto-plastic behaviors, the earthquake records are scaled. The scaled factors applied to the ground motions are 3 for El-Centro and 1.5 for Kobe ground motion respectively. In the dynamic analysis, the gravity loads are applied first and then hold constant while the seismic load is applied laterally in the direction of the 60 degrees angle from H1 axis.

In this model, modulus of elasticity, shear modulus and yield strength for steel are taken as 200 GPa, 81.5 GPa and 350 MPa, respectively. The 3D dynamic analysis is carried out using CSI software perform-3D. P-Δ and P-δ effects are both explicitly considered in this paper.
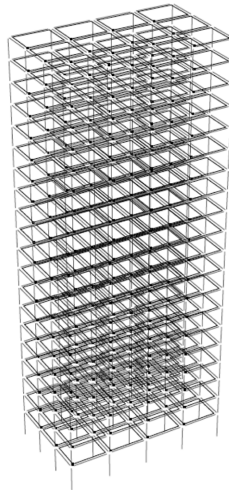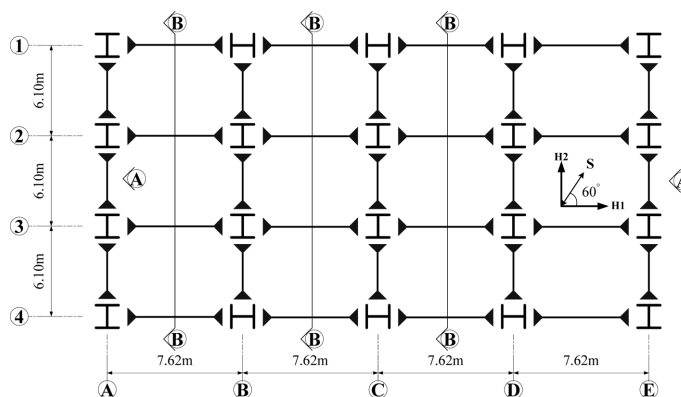

Fig. 1 The 3D space model
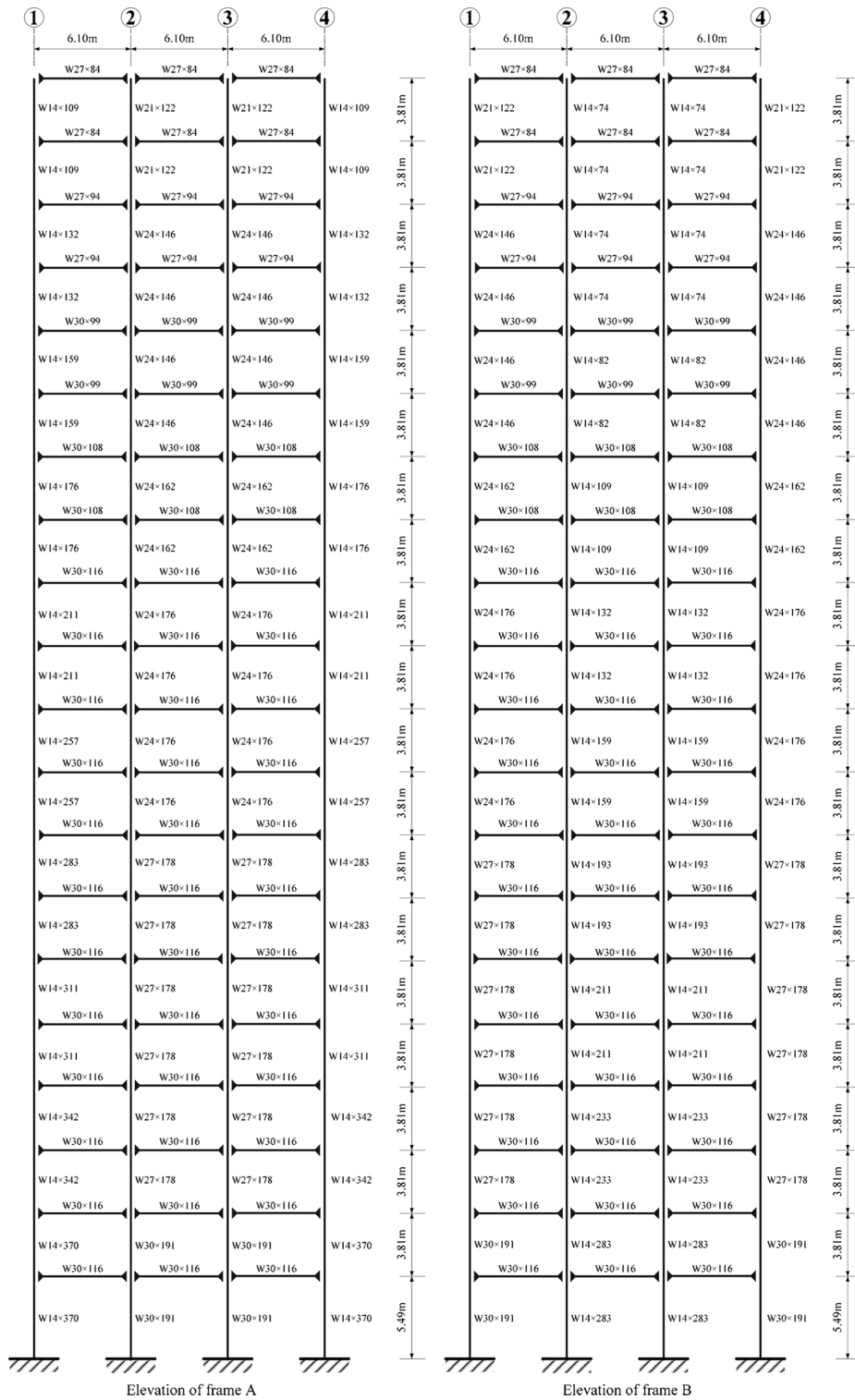

Fig. 2 Typical floor plan of the steel structure

Fig. 3 Elevation of frame A and B

Table 1 Characteristics of the earthquake waves

Earthquake	Record station	Component	PGA /g	Duration /sec	Scaled factor
IMPVALL, 1940	117 El Centro Array #9	I-ELC270	0.2148	25	3
Kobe, 1995	0 Takarazuka	TAZ000	0.6934	40.96	1.5

4.2 Finite element types for the structure

The structural beams and columns are modeled as FEMA-356 Beam/Column elements. The FEMA-356 Beam/Column element (FEMA 2000) is based on the chord rotation model and FEMA-356 gives specific guidelines for this model.

Each FEMA beam or column element has two components, namely a plastic hinge and an elastic segment, as illustrated in Fig. 4. The force-deformation relationships for the plastic hinges only are specified. At the ends of a member, it is common practice to assume that the region within the beam-to-column connection is stiffer than the body of the beam or column. Sometimes this region is assumed to be rigid. In this paper, this connection zone is assumed to be 10 times stiffer than the body of the beam or column. For columns, the interaction of axial force and moments is considered by means of default parameters for steel structures.

The elastic slab element is used to simulate floor slabs of the structure, which is a 4-node element with membrane (in-plane) and plate bending (out-of-plane) stiffness. The membrane behavior of the element accounts for in-plane effects of the floor slab, and the slab bending behavior can be used for applying and distributing gravity loads.
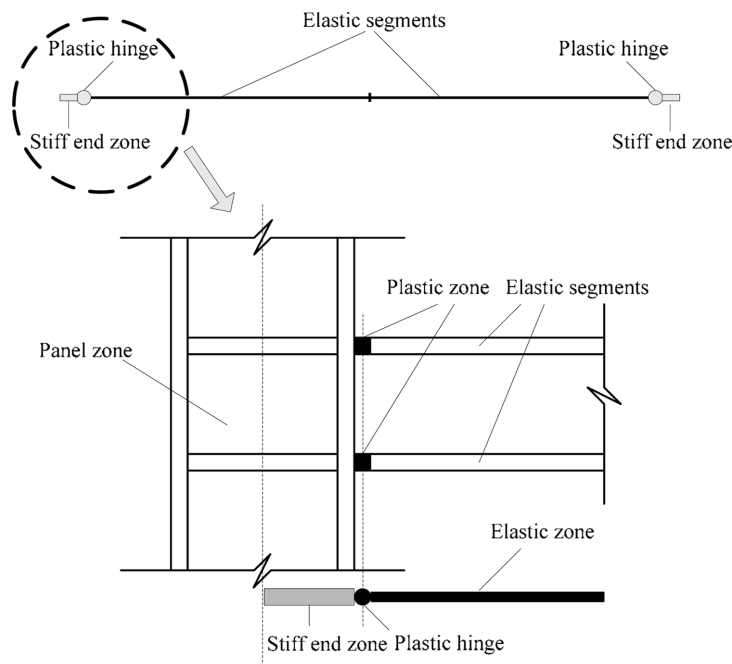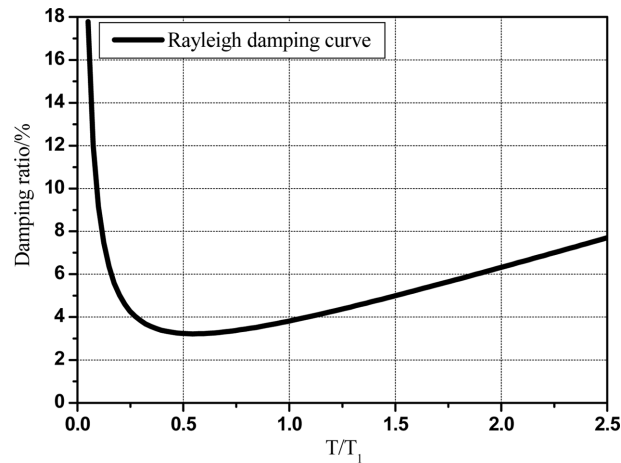

Fig. 4 FEMA beam/column element

Fig. 5 Rayleigh damping curve

4.3 Damping model for the structure

In the paper, Rayleigh damping model is used, and the additional damping due to the structure yielding is also taken into consideration. As a structure yields it usually softens, and hence its effective vibration periods usually increase. Period is inversely proportional to the square root of stiffness (based on secant stiffness). Hence, a ductility ratio of n corresponds roughly to a period increase of $n^{0.5}$. The proportionality factors α_m and β_k in Rayleigh model can be chosen to provide a defined percentage of critical damping at two specific periods of vibration. Reasonable periods to specify these damping values are $0.2T_1$ and $1.5T_1$, where T_1 is the fundamental period of vibration of the structure (NIST 2010). Based on observations and guidances in various documents (Charney 2008, Charney and Mc-Namara 2008), it is suggested to specify equivalent viscous damping in the range of 1% to 5% of critical damping over the range of periods from $0.2T_1$ to $1.5T_1$. These damping values are specified as 5% for both $0.2T_1$ and $1.5T_1$ in this paper. The Rayleigh damping curve is shown in Fig. 5.
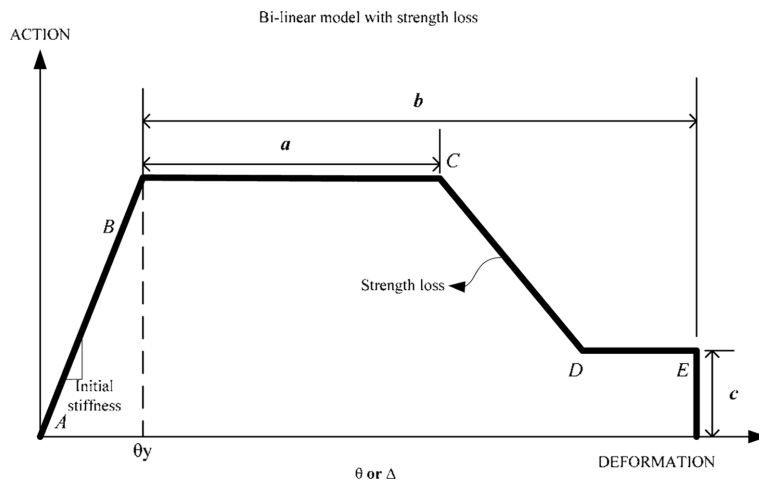

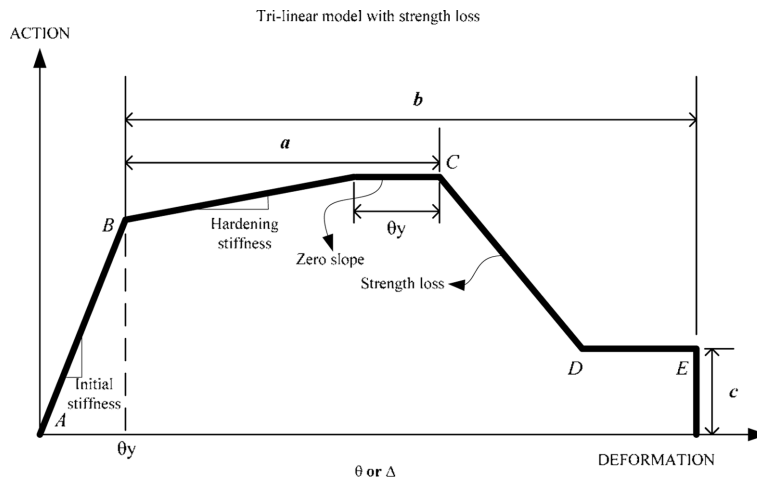Fig. 6 Bi-linear F-D relationship of a member with strength loss

Fig. 7 Tri-linear F-D relationship of a member with strength loss

4.4 Restoring force models of a member

The restoring force model describes the force-deformation relationship of a member. The F-D (force-displacement) relationship of a member under monotonic load can be used to clearly describe the restoring force characteristics and the characteristic parameters are obtained from observed experimental testing. In lieu of relationships derived from experiments, a bi-linear or tri-linear model with strength loss is the most commonly used for an elastio-plastic dynamic analysis (Akiyama 2010). The generalized load-deformation curves shown in Figs. 6 and 7, with parameters a, b, c, as defined in FEMA-356 (FEMA 2000), are used to characterize the nonlinear behavior of the steel members in this paper. The hardening stiffness in the tri-linear restoring force model is taken as 1% of the initial stiffness.

5. Analysis results

5.1 Influences of P-Δ/δ effects and restoring force models on energy components

Input energy and dissipated energy time histories under seismic excitations are shown in Fig. 8. It can be seen that the dissipated energy components, including viscous damping and hysteretic energy, increase with time, and reach the maximum at the end of the excitations. Therefore, it can be concluded that the duration of a strong motion affects the maximum viscous damping energy and hysteretic energy.

Fig. 8 shows that all the energy components are affected to various extents by P-Δ/δ effects, the energy values of the structure without consideration of P-Δ/δ effects are larger and a difference about 5~10% is observed.

The restoring force models have a minor effect on seismic input energy and the difference of less than 5% is observed, but they have a certain effect on viscous damping energy and hysteretic energy with the differences about 5~7% and 8~15% respectively. Viscous damping energy of the structure with the tri-linear restoring force model is smaller, while hysteretic energy is larger.
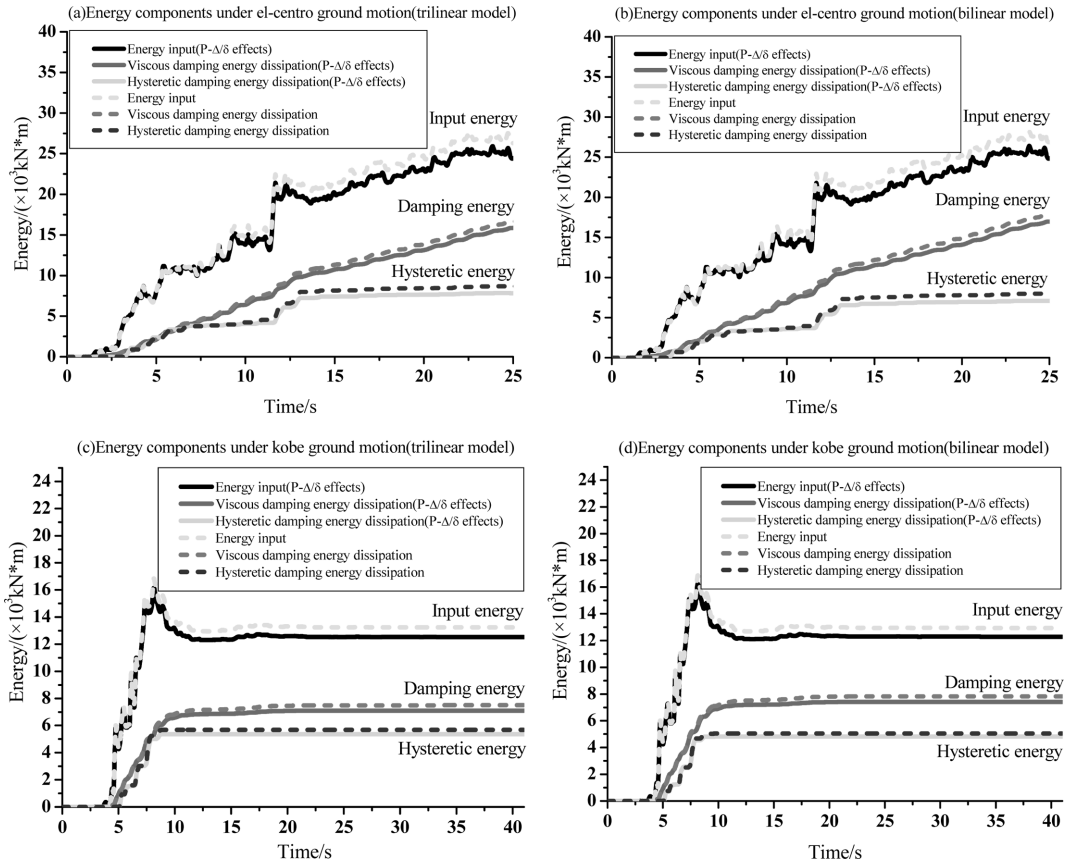
Fig. 8 Energy of the structure subjected to El-Centro and Kobe waves

The following parameters are defined as the dissipated energy ratios at the end of earthquakes.

$$r_v = E_\xi / E_I \tag{7}$$

$$r_h = E_h / E_I \tag{8}$$

in which r_v and r_h are the viscous damping energy ratio and hysteretic energy ratio, respectively. Based on Eqs. (7) and (8), the ratios are shown in Table 2.

Table 2 Energy ratios

	Tri-linear model				Bi-linear model			
	with P-Δ/δ effects		without P-Δ/δ effects		with P-Δ/δ effects		without P-Δ/δ effects	
	El-Centro	Kobe	El-Centro	Kobe	El-Centro	Kobe	El-Centro	Kobe
r_v	62.8%	56.7%	61.8%	56.5%	65.7%	60.4%	64.5%	60.8%
r_h	31.1%	43.1%	32.3%	42.5%	27.7%	39.3%	28.8%	38.9%
$r_v + r_h$	93.9%	99.8%	94.1%	99%	93.4%	99.7%	93.3%	99.7%

According to Table 2, it shows that P-Δ/δ effects and restoring force models have a minor effect on the ratios and the difference of less than 5% is observed. It also can be found that the most input energy is dissipated by damping and hysteretic action when the earthquake ends, only a small part of input energy, which can be ignored, is absorbed by kinetic energy and elastic strain energy. Therefore, the input energy, E_I, viscous damping energy, E_ξ, and hysteretic energy, E_h, have the following approximate relationship at the end of earthquake,

$$E_\xi + E_h \approx E_I \tag{9}$$

5.2 Influences of P-Δ/δ effects and restoring force models on inter-story hysteretic energy

Fig. 9 shows the inter-story hysteretic energy distribution along the height of the structure. It is observed that the restoring force models have a small influence on the inter-story hysteretic energy, while P-Δ/δ effects have an obvious effect on the inter-story hysteretic energies of stories with severely damaged members, such as the 1st floor of the structure subjected to the El-Centro earthquake excitation.

According to Fig. 9, the inter-story hysteretic energy distribution modes under different seismic excitations are approximately the same. Estes and Anderson (2002) found that the hysteretic energy

(a)Inter-story hysteretic energy under El-Centro ground motion

(b)Inter-story hysteretic energy under El-Centro ground motion

(c)Inter-story hysteretic energy under Northridge ground motion

(d)Inter-story hysteretic energy under Northridge ground motion
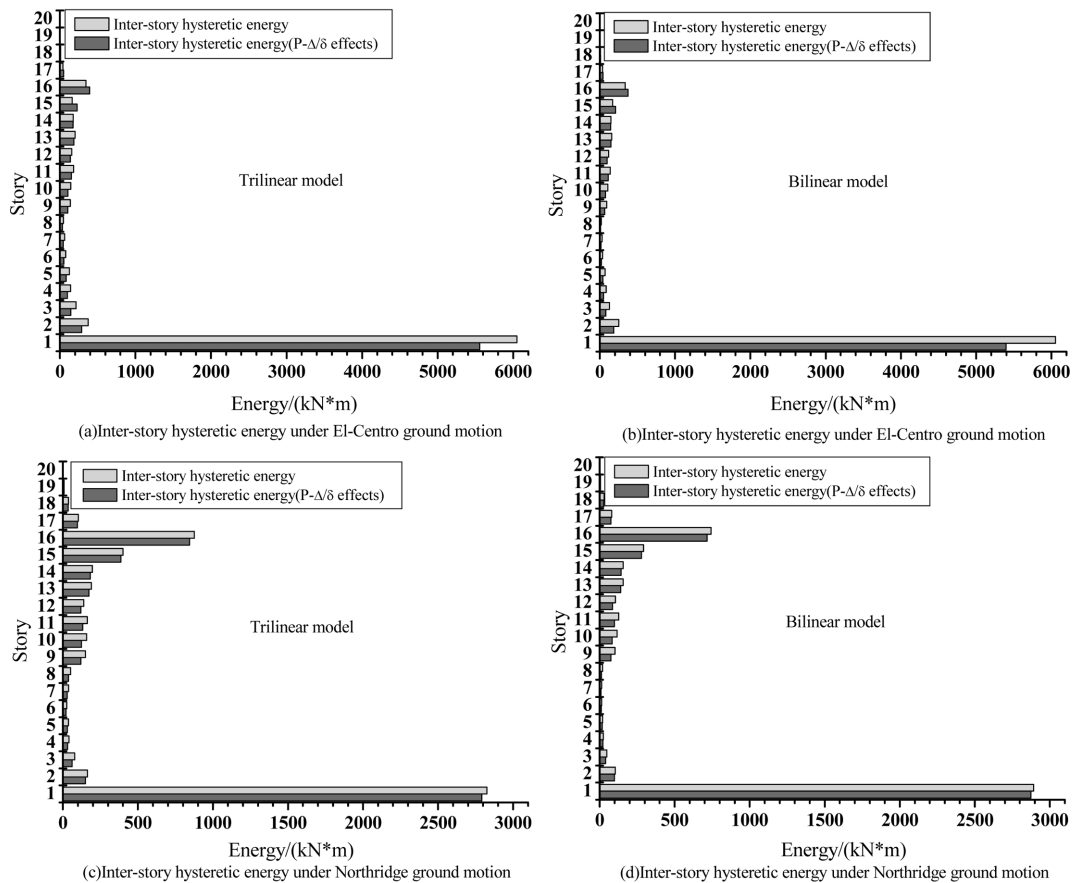
Fig. 9 Inter-story hysteretic energies

demand in each story of steel moment frames is the largest in the first story and decreases linearly in higher stories. In this paper, it is found that the inter-story hysteretic energy demands under these earthquake excitations are the largest in the first floor, but not always decrease with height; they decrease at beginning, then increase, finally decrease. The inter-story hysteretic energies have a complex distribution pattern for the high-rise building.

The inter-story hysteretic energy reflects the story damage degree. It can be seen from Fig. 9 that the members at the 1st floor are most severely damaged, and the contribution to total hysteretic energy is mainly from these members, where the hysteretic energy accounts for about 50% of the total hysteretic energy. The members from the 4th to the 9th and the 17th to the 20th have a minor damage.

5.3 Energy ratio time histories

Fig. 10 shows the time-histories about the viscous damping energy and hysteretic energy ratios of the structure with tri-linear restoring force model together with consideration of P-Δ/δ effects. It shows that the time-histories of the viscous damping energy ratios have large oscillations at the beginning of excitations and the maximum viscous damping energy ratios occur at the end of excitations, when about 68% and 57% of the overall seismic input energy are dissipated, while the maximum hysteretic energy ratios occur at 7s and 12s, when about 38% and 43% of the seismic input energy are dissipated.
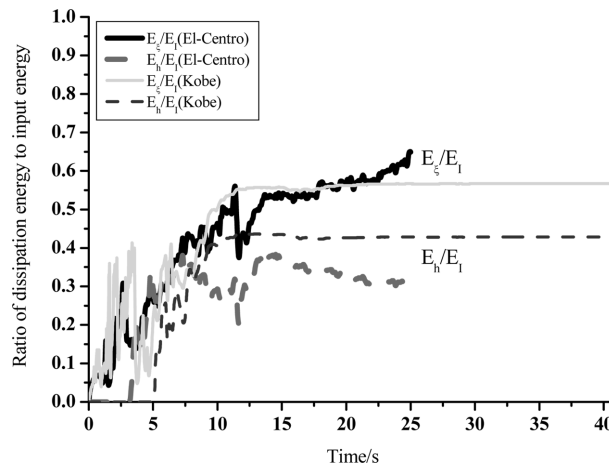

Fig. 10 Ratios of dissipation energy components to input energy

Table 3 Equivalent pseudo-velocities of energy components

| | Tri-linear model | | | | Bi-linear model | | | |
| | with P-Δ/δ effects | | without P-Δ/δ effects | | with P-Δ/δ effects | | without P-Δ/δ effects | |
	El-Centro	Kobe	El-Centro	Kobe	El-Centro	Kobe	El-Centro	Kobe
V_i/m/s	2.49	1.91	2.71	2.12	2.61	1.93	2.72	2.14
V_h/m/s	2.08	2.11	2.55	2.47	2.02	2.03	2.43	2.39
V_E/m/s	3.30	2.84	3.74	3.25	3.29	2.81	3.70	3.21
V_h/ V_E	63%	74%	69%	76%	61%	72%	66%	74%
Limit PGA	0.751g	1.421g	0.859g	1.546g	0.751g	1.387g	0.831g	1.525g

5.4 Equivalent pseudo-velocities at ultimate state of load carrying capacity

Akiyama (1985) expressed E_I in terms of equivalent pseudo-velocity, V_E, which is defined as follow

$$V_E = \sqrt{\frac{2E_I^*}{M}} \tag{10}$$

in which $E_I^* =$ input energy value; $M =$ total mass. Equivalent pseudo-velocities of other energy components can also be written as the above expression.

By adjusting peak accelerations of the earthquake records, equivalent pseudo-velocities, V_ξ, V_h and V_E, of viscous damping energy, hysteretic damping energy and seismic input energy at the ultimate state can be obtained by means of the above equation, as shown in Table 3.

From Table 3, their relationships of the equivalent velocities are as follows

$$V_{\xi\,t,\,w} < V_{\xi,\,b,\,w} < V_{\xi\,t,\,o} < V_{\xi,\,b,\,o}$$
$$V_{h,\,b,\,w} < V_{h,\,t,\,w} < V_{h,\,b,\,o} < V_{h,\,t,\,o}$$
$$V_{E,\,b,\,w} < V_{E,\,t,\,w} < V_{E,\,b,\,o} < V_{E,\,t,\,o}$$

where $t =$ tri-linear model; $b =$ bi-linear model; $w =$ with consideration of P-Δ/δ effects; $o =$ without consideration of P-Δ/δ effects.

It can be observed from this table that, for the given seismic record, the effects of different restoring models on the equivalent pseudo-velocities are minor, but when P-Δ/δ effects are considered, V_ξ, V_h or V_E has a considerable change, and it also can be found that V_h is a relatively stable value at the ultimate state for the two seismic excitations when P-Δ/δ effects is considered or not. Thus, the $V_h = V_{max}$ or $E_h = E_{h,\,max}$ can be regarded as the seismic capacity evaluation parameter of a structure, but it still needs to be investigated in depth by using a large number of earthquakes recorded.

5.5 Seismic capacity evaluation

In this paper, the seismic input energy, E_I, and the plastic hysteretic energy, E_h, are used to evaluate the seismic capacity of the structure respectively. $E_{I,\,d}/E_{I,\,c}$ (Demand-Capacity Ratio of input energy) and $E_{h,\,d}/E_{h,\,c}$ (Demand-Capacity Ratio of hysteretic energy) time histories are shown as Fig. 11.

It can be noted that the curves are approximately steady after reaching the maximum. P-Δ/δ effects have a remarkable influence on the ratios, and a difference of 10~15% is observed. The ratios increase due to consideration of P-Δ/δ effects, while the restoring model has a weak effect on them.

6. Relationship between damping and energy dissipation

6.1 Equivalent damping ratios of the structure

For a SDOF structure subjected to earthquake loading, the strain energy varies with time and each strain energy peak corresponds to a half cycle. If the dissipated energy is known for a whole number of half cycles, assuming that the mean of the strain energy peaks is 2 times of the mean strain energy, the equivalent damping ratio can be calculated as follows (Computer & Structure, INC. 2006)
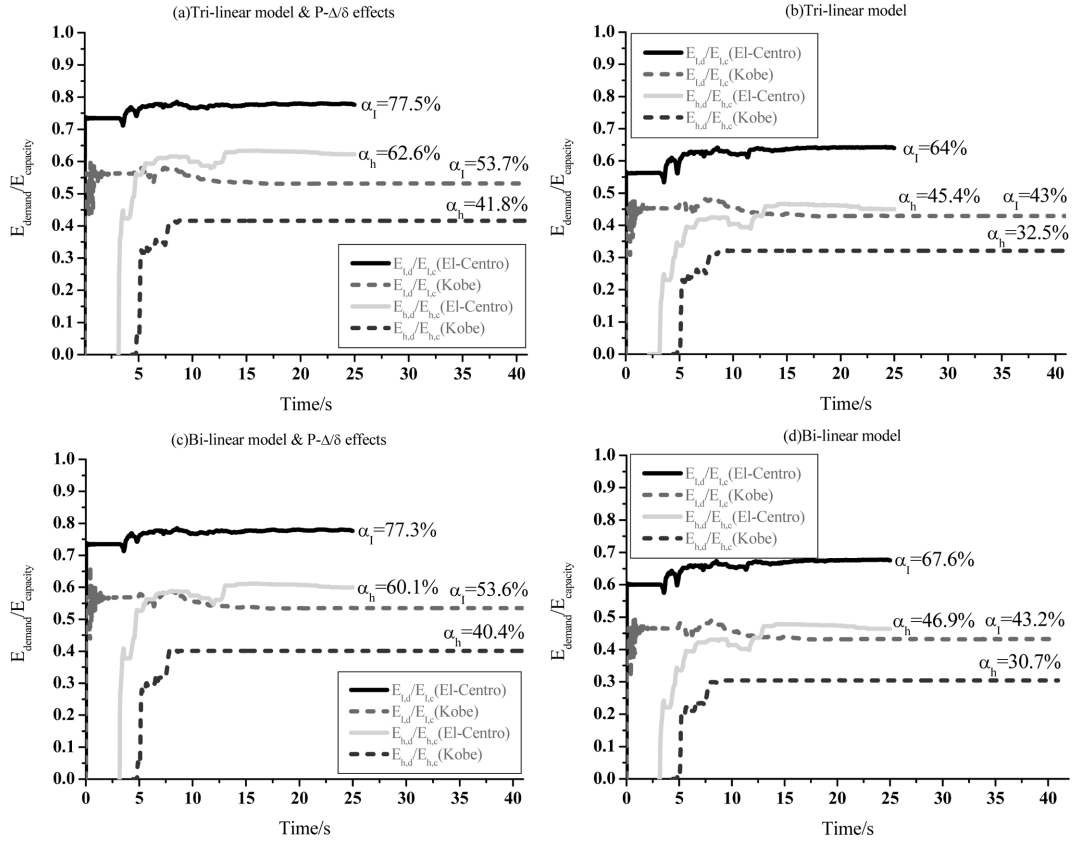
Fig. 11 Seismic capacity evaluation of the structure

$$\xi \;=\; \frac{1}{2\pi N}\frac{E_d}{E_{ms}} \tag{11}$$

Where ξ = damping ratio; E_d = dissipated energy in structure; N = number of half cycles (strain energy peaks), E_{ms} = mean of strain energy peaks.

For a MDOF nonlinear structure the strain energy variation is complex, however, a rough estimation of the effective damping ratio can be calculated as

$$\xi \;=\; \frac{1}{2\pi N}\frac{E_d}{2E_m} \tag{12}$$

in which it is assumed that the mean of the strain energy peaks, E_{ms}, is 2 times of the mean strain energy, E_m.

The paper investigates the variations in equivalent viscous and hysteretic damping ratios of the structure with ground motion intensities, as shown in Fig. 12.

From Fig. 12, it shows that the equivalent viscous damping ratios change little with scale factors of the ground motions. However, the equivalent hysteretic damping ratios approximately increase linearly
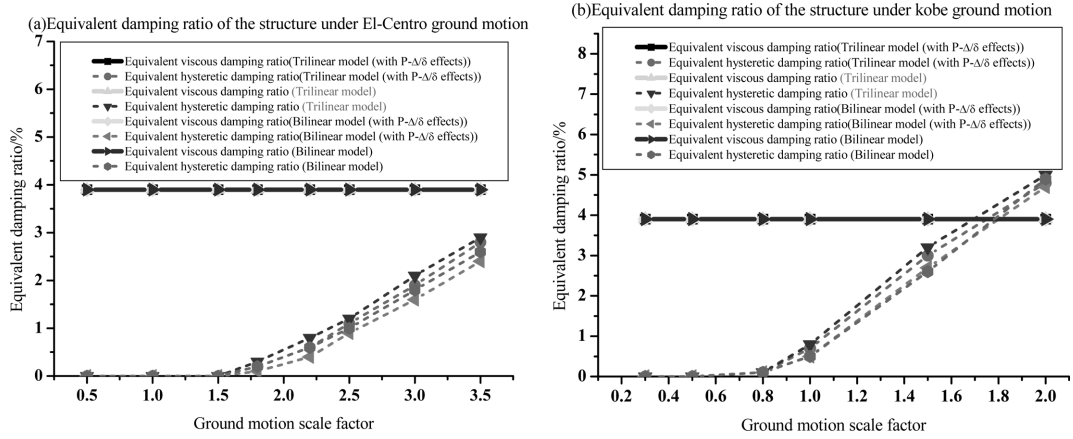
Fig. 12 Equivalent damping ratios of different ground motion intensities

with scale factors in elastio-plastic stage. P-Δ/δ effects and restoring force models have no effect on the equivalent viscous damping ratios. The equivalent hysteretic damping ratios are less about 10% due to considering P-Δ/δ effects, while the use of tri-linear restoring force model results in an increase of about 15%.

According to Fig. 12, the total equivalent damping ratio of the structure can be written as

$$\xi_t^{eq} = \begin{cases} \xi_1 & \textit{for elastic stage} \\ \xi_1 + \xi_h^{eq} & \textit{for elasto-plastic stage} \end{cases}$$

where ξ_t^{eq} = total equivalent damping ratio; ξ_1 = equivalent viscous damping ratio; ξ_h^{eq} = equivalent hysteretic damping ratio.
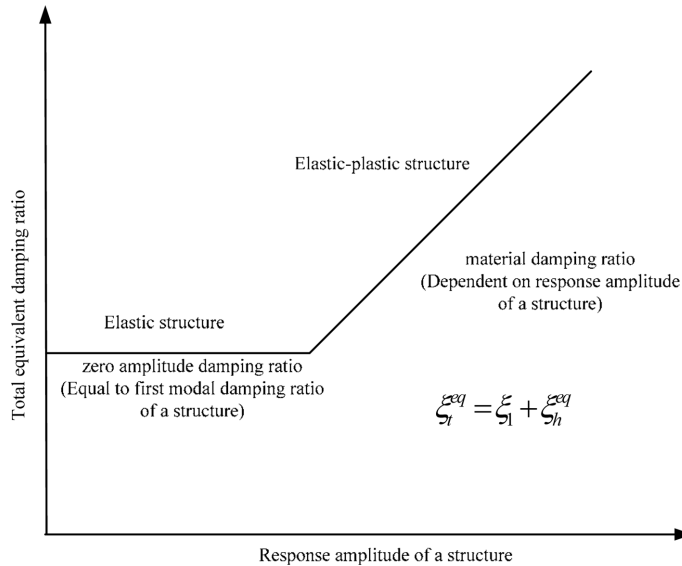

Fig. 13 Total equivalent damping curve

The above equation is illustrated in Fig. 13. Total damping ratio consists of two parts according to structural global response amplitude. One is the equivalent viscous damping ratio in elastic stage, which is a constant and equal to the first mode damping ratio of the structure, also called "zero amplitude damping ratio"; the other is the equivalent hysteretic damping ratio, which approximately increases linearly with structural global response amplitude. Hysteretic analysis (or other approximations) can be used to estimate an equivalent hysteretic damping ratio of a structure at the target ductility. The amplitude-dependent damping model proposed in this paper can be used in dynamic analysis, and it makes the structural designers have a deeper understanding for damping characteristics of a structure.

6.2 Ratios of dissipated energy components to input energy

The ratios of dissipated energy components to seismic input energy under different ground motion intensities are shown in Fig. 14. It shows that the energy dissipation completely depends on viscous damping in elastic stage, while the seismic input energy is dissipated by both in elastio-plastic stage. The viscous damping dissipation energy ratios approximately decrease linearly with ground motion intensities after the hysteretic dissipation energy arises, but it is contrary to the hysteretic dissipation energy ratios. Both P-Δ/δ effects and restoring force models have a minor effect on the ratios with a difference of less than 5%.

The percentage of hysteretic energy which induced structural damage to input energy is proposed as follow (Akiyama 2010)

$$E_D = \frac{1}{\left(1 + 3h + 1.2\sqrt{h}\right)^2} E_I \qquad (13)$$

where E_D = hysteretic energy inducing structural damage; h = critical damping ratio;

The hysteretic energy is estimated by the critical damping ratio in Eq. (13), which is a design parameter in engineering practice (Akiyama 2010). In this paper, a simple evaluation method for the ratio of dissipated energy to input energy is proposed. According to Eq. (12), the equivalent viscous damping and hysteretic damping ratios are, respectively, written as
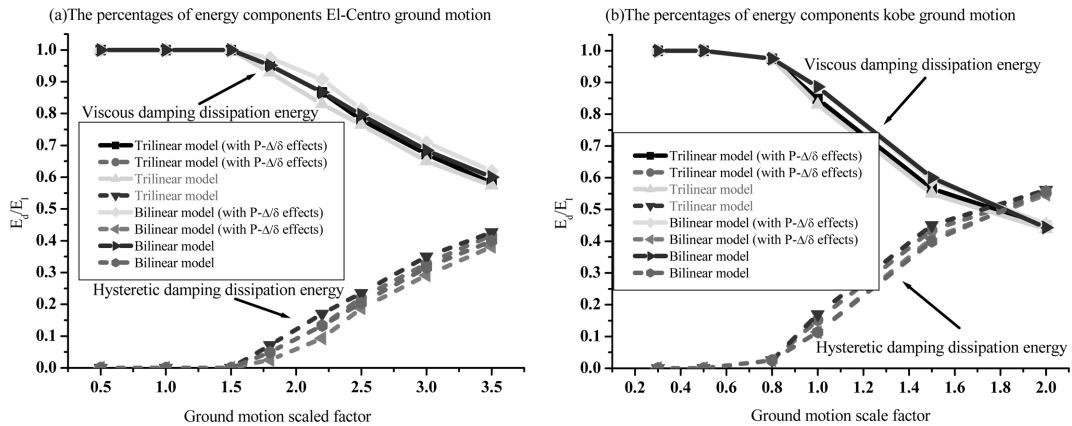

Fig. 14 Viscous damping energy and hysteretic damping to energy input

$$\xi_v = \frac{1}{2\pi N}\frac{E_\xi}{2E_m} \tag{14}$$

$$\xi_h = \frac{1}{2\pi N}\frac{E_h}{2E_m} \tag{15}$$

where ξ_v = equivalent viscous damping ratio; ξ_h = equivalent hysteretic damping ratio.
According to Eqs. (14) and (15), the following equation can be obtained

$$\frac{\xi_v}{\xi_h} = \frac{E_\xi}{E_h} \tag{16}$$

Assuming that initial strain energy due to gravity load is ignored, when the earthquake ended, according to Eqs. (9) and (16), it has

$$E_h = \frac{\xi_h}{\xi_1 + \xi_h}E_I \tag{17}$$

Note that

$$\xi_v = \xi_1$$

Therefore, hysteretic energy can be calculated as

$$E_h = \frac{\xi_h}{\xi_1 + \xi_h}E_I$$

The ratios of viscous damping and hysteretic damping energy dissipation to total input energy are $\gamma_v = \xi_1/\xi_1+\xi_h$ and $\gamma_h = \xi_h/\xi_1+\xi_h$, respectively.

Take $\xi_t = \xi_1 + \xi_h$, $\xi_1 = 0.039$ into consideration in this paper, $\gamma_v - \xi_t$ and $\gamma_h - \xi_t$ curves can be described as illustrated in Fig. 15.
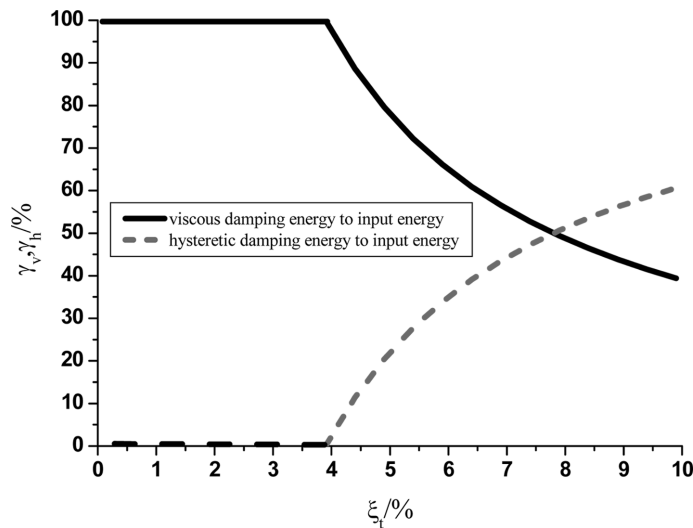

Fig. 15 $\gamma_v - \xi_t$ and $\gamma_h - \xi_t$ curves

7. Conclusions

This paper uses energy balance concept to analyze the seismic nonlinear behaviors of a high-rise steel structure, and the main factors such as P-Δ/δ effects and different restoring force models affecting the seismic performance of a high rise structure are taken into consideration. A new amplitude-dependent damping model, which combines the equivalent viscous damping and hysteretic damping ratios of the structure subjected to strong ground motions, is discussed. Two typical ground motions records are used for the study and the limited results are obtained from this typical structure, but they also allow us to draw some important conclusions for high-rise structure design purposes. Although seismic design mechanism based on energy is largely accepted, there are large differences between energy indices and conventional strength and ductility indices and it is still very difficult to establish the appropriate calculation method and design theory. Seismic analysis based on energy balance need to make a thorough study in the future.

Acknowledgments

References

Akiyama, H. (1985), *Earthquake-resistant limit-state design for buildings*, The University of Tokyo Press, Tokyo.

Akiyama, H. (2010), *Earthquake-resistant design method for buildings based on energy balance*, Tsinghua University Press,Beijing, China. (In Chinese)

Aschheim, M. and Montes, E.H. (2003), "The representation of P-Δ effects using yield point spectra", *Eng. Struct.*, **25**(11),1387-1396.

Bojórquez, E., Reyes-Salazar, A., Terán-Gilmore, A. and Ruiz, S.E. (2010), "Energy-based damage index for steel structures", *Steel and Composite Structure*, **10**(4), 343-360.

Bojórquez, E., Ruiz, S.E. and Terán-Gilmore, A. (2008), "Reliability-based evaluation of steel structures using energy concepts", *Eng. Struct.*, **30**(6), 1745-1759.

Bruneau, M. and Wang, N. (1996), "Some aspects of energy methods for the inelastic seismic response of ductile SDOF structures", *Eng. Struct.*, **18**(1), 1-12.

Charney, F.A. (2008), "Unintended consequences of modeling damping in structures", *J. Struct. Eng.*, *ASCE*, **134** (4), 581-592.

Charney, F.A. and McNamara, R.J. (2008), "A method for computing equivalent viscous damping ratio for structures with added viscous damping", *J. Struct. Eng.*, *ASCE*, **134**(1), 32-44.

Chen, S.J. and Wang, W.C. (1999), "Moment amplification factor for P-δ effect of steel beam-column", *J. Struct. Eng.*, *ASCE*, **125**(2), 219-223.

Choi, H.H and Kim, J.K. (2009), "Evaluation of seismic energy demand and its application on design of buckling-restrained braced frames", *Struct. Eng. Mech.*, **31**(1), 93-112.

Chopra, A.K. (1995), *Dynamics of Structures: Theory and Applications to Earthquake Engineering,* Prentice Hall Inc., New Jersey.

Chopra, A.K.and Goel, R.K. (2002), "A modal pushover analysis procedure for estimating seismic demands for buildings", *Earthquake Engineering & Structural Dynamics*, **31**(3), 561-582.

Chou, C.C. and Uang, C.M. (2003), "A procedure for evaluating seismic energy demand of framed structures", *Earthquake Engineering & Structural Dynamics*, **32**(2), 229-244.

Computer & Structure, INC. (2006), "Perform 3D User Guide: Nonlinear Analysis and Performance Assessment for 3D Structures", Berkeley, California.

Decanini, L.D. and Mollaioli, F. (2001), "An energy-based methodology for the seismic assessment of seismic demand", *Soil Dynamics and Earthquake Engineering*, **21**(2), 113-137.

Estes, K.R. and Anderson, J.C. (2002), "Hysteretic energy demands in multistory buildings", *Seventh U.S. National Conference on Earthquake Engineering*, Boston, July.

Fajfar, P and Fischinger, M. (1990), "A seismic procedure including energy concept", *Proceedings of IX ECEE*, Moscow, September.

Fajfar, P. and Gašperšič, P. (1996), "The N2 method for the seismic damage analysis of RC buildings", *Earthq. Eng. Struct. Dyn.*, **25**(1), 31-46.

Fajfar, P. and Vidic, T. (1994), "Consistent inelastic design spectra: hysteretic and input energy", *Earthq. Eng. Struct. Dyn.*, **23**(5), 523-537.

Fajfar, P., Vidic, T. and Fischinger, M. (1989), "Seismic demand in medium- and long-period structures", *Earthq. Eng. Struct. Dyn.*, **18**(8), 1133-1144.

FEMA. (2009a), Effects of strength and stiffness degradation on seismic response, FEMA Report 440a, Washington, D.C.

FEMA. (2009b), Quantification of building seismic performance factors, FEMA Report P695, Washington, D.C.

FEMA. (2000), Pre-standard and commentary for the seismic rehabilitation of buildings, FEMA Report 356, Washington, D.C.

Gaetano, M. (2001), "Evaluation of seismic energy demand", *Earthq. Eng. Struct. Dyn.*, **30**(4), 485-499.

Jawahar, M.T. and James, M.N. (1987), "Inelastic modeling and seismic energy dissipation", *J. Struct. Eng.*, *ASCE*, **113**(6), 1373-1377.

Leelataviwat, S., Goel, S.C. and Stojadinovi, B. (2002), "Energy-based seismic design of structure using yield mechanism and target drift", *J. Struct. Eng.*, *ASCE*, **128**(8), 1046-1054.

Nassar, A. and Krawinkler, H. (1991), "Seismic Demands for SDOF and MDOF systems", Report No. 95, The John A. Blume Earthquake Engineering Center, Stanford University.

NIST. (2010), "Nonlinear Structural Analysis For Seismic Design: A Guide for Practicing Engineers", NIST GCR 10-917-5, Prepared for U.S. Department of Commerce Building and Fire Research Laboratory National Institute of Standards and Technology, Gaithersburg, MD.

PEER/ATC. (2010), Modeling and Acceptance Criteria for Seismic Design and Analysis of Tall Buildings. PEER/ATC 72-1 Report, Applied Technology Council, Redwood City, CA.

Prasanth, T., Ghosh, S. and Collins, K.R. (2008), "Estimation of hysteretic energy demand using concepts of modal pushover analysis", *Earthquake Engineering & Structural Dynamics*, **37**(6), 975-990.

Reyes-Salazar, A. and Haldar, A. (2001), "Seismic Response and Energy Dissipation in Partially Restrained and Fully Restrained Steel Frames: An Analytical Study", *Steel and Composite Structures*, **1**(4), 459-480.

Safac, E. (2000), "Characterization of seismic hazard and structural response by energy flux", *Soil Dynamics and Earthquake Engineering*, **20**(1-4), 39-43.

Shen, J. and Akbas, B. (1999), "Seismic energy demand in steel moment frames", *J. Earthq. Eng.*, **3**(4), 519-559.

Somerville, P., Smith, H., Puriyamurthala, S. and Sun, J. (1997), "Development of ground motion time histories for phase 2 of the FEMA/SAC steel project", SAC Joint Venture, SAC/BD-97/04.

Uang, C.M. and Bertero, V.V. (1990), "Evaluation of seismic energy in structures", *Earthq. Eng. Struct. Dyn.*, **19**(1), 77-90.

Williamson, E.B. (2003), "Evaluation of damage and P-Δ effects for systems under earthquake excitation", *J. Struct. Eng.*, *ASCE*, **129**(8), 1036-1046.

Zahrah, T.F. and Hall, W.J. (1984), "Earthquake energy absorption in SDOF structures", *J. Struct. Eng.*, *ASCE*, **110**(8), 1757-1772.

CC